Hindawi Publishing Corporation
Advances in Optical Technologies
Volume 2014, Article ID 958327, 8 pages
http://dx.doi.org/10.1155/2014/958327

Hindawi

Research Article

Emission Spectral Control of a Silicon Light Emitting Diode Fabricated by Dressed-Photon-Phonon Assisted Annealing Using a Short Pulse Pair

Tadashi Kawazoe,[1,2] Naoki Wada,[1] and Motoichi Ohtsu[1,2]

[1] *Department of Electrical Engineering and Information Systems, Graduate School of Engineering, The University of Tokyo, 2-11-16 Yayoi, Bunkyo-ku, Tokyo 113-8656, Japan*
[2] *Nanophotonic Research Center, Graduate School of Engineering, The University of Tokyo, 2-11-16 Yayoi, Bunkyo-ku, Tokyo 113-8656, Japan*

Correspondence should be addressed to Tadashi Kawazoe; kawazoe@ee.t.u-tokyo.ac.jp

Received 24 April 2014; Accepted 5 June 2014; Published 6 July 2014

Academic Editor: Takashi Yatsui

We fabricated a high-efficiency infrared light emitting diode (LED) via dressed-photon-phonon (DPP) assisted annealing of a p-n homojunctioned bulk Si crystal. The center wavelength in the electroluminescence (EL) spectrum of this LED was determined by the wavelength of a CW laser used in the DPP-assisted annealing. We have proposed a novel method of controlling the EL spectral shape by additionally using a pulsed light source in order to control the number of phonons for the DPP-assisted annealing. In this method, the Si crystal is irradiated with a pair of pulses having an arrival time difference between them. The number of coherent phonons created is increased (reduced) by tuning (detuning) this time difference. A Si-LED was subjected to DPP-assisted annealing using a 1.3 μm ($h\nu$ = 0.94 eV) CW laser and a mode-locked pulsed laser with a pulse width of 17 fs. When the number of phonons was increased, the EL emission spectrum broadened toward the high-energy side by 200 meV or more. The broadening towards the low-energy side was reduced to 120 meV.

1. Introduction

Direct transition type semiconductors are mainly used in semiconductor light emitting diodes (LEDs) [1, 2]. The reason for this is that the probability of electric dipole transitions, in other words, the radiative recombination probability, is high. Also, the emission wavelength is determined by the bandgap energy, E_g, of the material used. Therefore, for example, InGaAsP epitaxially grown on an InP substrate is mainly used as the active layer for near-infrared LEDs with emission wavelengths of 1.00–1.70 μm (0.73–1.24 eV), which includes the optical fiber communication wavelength band. Shortcomings with this approach are that InP is highly toxic [3], and In is a rare resource. Silicon (Si), on the other hand, is a semiconductor having low toxicity and no concerns about depletion of resources; however, its emission efficiency is low since it is an indirect transition type semiconductor. Therefore, Si is usually not suitable as a material for use in LEDs. Nevertheless, there is a great demand for the use of Si in light emitting devices, and there has been extensive research into improving its emission efficiency. For example, there has been research into making Si emit light in the visible region by utilizing the quantum size effect of Si and by using porous Si [4], a Si/SiO_2 superlattice structure [5, 6], and Si nanoprecipitates in SiO_2 [7], as well as research into making Si emit light in the near-infrared region by doping it with light-emitting materials, such as erbium (Er)-doped Si [8] and silicon-germanium (Si-Ge) [9]. However, the reported external quantum efficiencies and power conversion efficiencies of LEDs using these materials have been low, at 0.5% and 0.8%, respectively [10].

On the other hand, using a homojunction-structured Si bulk crystal, we realized a high-efficiency, wideband LED in which the spatial distribution of the dopant density in

the Si was modified via a novel process of dressed-photon-phonon assisted annealing (DPP-assisted annealing) [11], and we achieved an external quantum efficiency of 40% and a power conversion efficiency of 50% [12]. A dressed photon (DP) is a quasi-particle created when a photon couples with an electron-hole pair in a nanometric region. Similarly, a dressed-photon-phonon (DPP) is a quasi-particle created when a DP couples with a phonon in a nanometric region. We have also succeeded in developing a Si laser [13], an infrared Si photodetector [14], and a Si relaxation oscillator [15], by using DPP-assisted annealing. These devices operate based on transitions mediated by DPPs, and the center wavelength of the electroluminescence (EL) spectrum is determined by the wavelength of the light source used for creating the DPPs. Since a DPP is a state in which a DP is coupled with a phonon in the material, the EL spectrum of the Si-LED described above has a large number of sidebands that are regularly arranged with a spacing corresponding to the optical phonon energy, centered on the photon energy of the light used in the DPP-assisted annealing. These sidebands are caused by coherent phonons (CPs) contributing to light emission. In typical light emitting devices, such sidebands originating from phonons (phonon sidebands) are observed in the photoluminescence spectrum, but are not observed in the EL spectrum. The observation of such sidebands in the EL spectrum, as described above, is a phenomenon unique to LEDs fabricated using DPPs. By using this phenomenon, it is possible to control the shape of the EL spectrum of a Si-LED by controlling the number of CPs created during the DPP-assisted annealing. In this paper, we report the results of our experiments in which we succeeded in controlling the generation of CPs by using a pair of pulses during the DPP-assisted annealing, allowing us to control the shape of the emission spectrum of a Si-LED.

2. Si-LED Fabrication and Principle of Sideband Creation

First, for fabricating a Si-LED, ion implantation is used to form an inhomogeneous spatial distribution of the dopant (boron: B) in a Si p-n homojunction substrate. Although the inhomogeneously concentrated B serves as the origin of the created DPPs, the created DPPs are not converted to propagating light that is detected outside the LED. However, if DPP-assisted annealing is used, it is possible to modify the spatial distribution of the B concentration so that the DPPs are converted to propagating light with high efficiency [12]. In the DPP-assisted annealing, a Si p-n homojunction substrate is irradiated with CW laser light while applying a forward-bias current, to control the thermal diffusion rate of the B. With this method, it has been demonstrated that the emission wavelength of a Si-LED does not depend on the bandgap energy, E_g, of the material used, but is determined by the photon energy, $h\nu_{\text{anneal}}$, of the radiated light [16]. In the present work, we performed DPP-assisted annealing by radiating CW laser light having a photon energy ($h\nu_{\text{anneal}} = 0.94\,\text{eV}$) lower than E_g of silicon ($= 1.14\,\text{eV}$). The principle will be described below. For more details, refer to [12].

During DPP-assisted annealing, the radiated light is not absorbed by the Si crystal at positions in the B distribution where DPPs are not created under irradiation. Thus, the energy of the electrons injected from the forward bias current is converted to thermal energy and is subsequently dissipated via intraband relaxation or nonradiative relaxation. Therefore, the B distribution randomly varies due to thermal diffusion. On the other hand, at positions where DPPs are readily created, the radiated light interacts with electron-hole pairs and phonons, whereby DPPs are created. In this case, the injected electrons emit propagating light via stimulated emission driven by localized DPPs. In other words, since part of the energy of the injected electrons is dissipated not in the form of thermal energy but in the form of optical energy, thermal diffusion becomes more difficult. In the two processes described above, the B concentration distribution in the Si crystal is modified, in a self-organized manner, to a structure suitable for the creation of DPPs and their subsequent conversion to propagating light, and then reaches an equilibrium state. The B distribution in this state is suitable for stimulated emission with the photon energy of the light irradiation, $h\nu_{\text{anneal}}$, and since the spontaneous emission probability is proportional to the stimulated emission probability, this p-n homojunction functions as a Si-LED that emits propagating light.

Next, the mechanism of sideband creation will be explained. Figure 1(a) is an energy level diagram showing electronic states in a Si-LED fabricated by DPP-assisted annealing, and Figure 1(b) is a diagram in which an intermediate DPP level has been added to the band structure. The state $|E_g; \text{el}\rangle \otimes |E_{\text{ex}}; \text{phonon}\rangle$ in the figure is a state represented by the direct product of the ground state $|E_g; \text{el}\rangle$ of the electron and the excited phonon state $|E_{\text{ex}}; \text{phonon}\rangle$. Transitions to this state $|E_g; \text{el}\rangle \otimes |E_{\text{ex}}; \text{phonon}\rangle$ have been shown to occur only due to absorption or emission of photons via DPPs [11]. When this is illustrated in the electronic band structure, it is a localized state in which DPP-mediated excitation can take place and, therefore, it is indicated by a constant-energy straight line (horizontal solid or broken line), as shown in Figure 1(b), due to wavenumber uncertainty. Although an adequate explanation of the conventional light emission process in Si-LEDs has been possible until now with only Figure 1(a), Figure 1(b) is also presented in the present paper to emphasize the significance of phonons. In the light emission process of Si-LEDs, since electrons are excited to the state $|E_{\text{ex}}; \text{el}\rangle$ by current injection, the initial state $|E_{\text{ex}}; \text{el}\rangle \otimes |E_{\text{ex}_{\text{thermal}}}; \text{phonon}\rangle$ in the light emission process exists close to the X point in the conduction band in Figure 1(b). Here, $|E_{\text{ex}_{\text{thermal}}}; \text{phonon}\rangle$ is the thermally excited state of the phonon. Similarly, since the final state $|E_g; \text{el}\rangle \otimes |E_{\text{ex}_{\text{thermal}}}; \text{phonon}\rangle$, reached after the light emission, corresponds to the energy state of holes created by the injected current, the state $|E_g; \text{el}\rangle$ concentrates in the vicinity of the Γ point at the top of the valence band. The state $|E_{\text{ex}_{\text{thermal}}}; \text{phonon}\rangle$ is limited to phonons that can exist at room temperature, according to Bose statistics. In other words, the states $|E_{\text{ex}}; \text{el}\rangle \otimes |E_{\text{ex}_{\text{thermal}}}; \text{phonon}\rangle$ and $|E_g; \text{el}\rangle \otimes |E_{\text{ex}_{\text{thermal}}}; \text{phonon}\rangle$ are the initial state and the final state in the usual indirect transition.

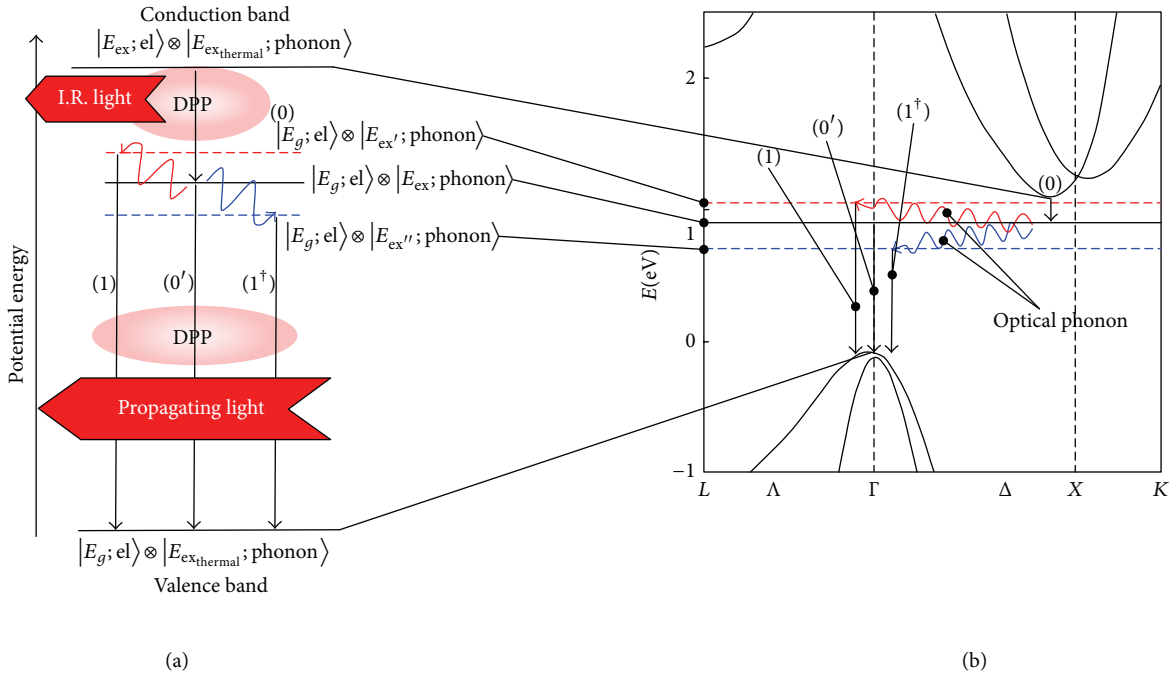

FIGURE 1: Diagram for explaining DPP-mediated transitions, showing (a) energy levels and (b) levels that can be reached via DPP-mediated transitions in electronic band structure of Si crystal.

Next, the processes (0), (0′), (1), and (1†) in Figure 1 will be explained. As the first-step, process (0) occurs. Processes (0′), (1), and (1†) occur as the second step. These processes involve externally observable transitions, in other words, photon emission. Processes (0) and (0′) are transitions that do not require a phonon, whereas processes (1) and (1†) require an optical phonon. Similarly, (n) and ($n^{\dagger}$) are transitions involving n optical phonons ($n = 2, 3, 4, \ldots$).

Process (0) is the first-step transition from the initial state $|E_{ex};el\rangle \otimes |E_{ex_{thermal}};phonon\rangle$ of electrons injected near the X point by the current to the intermediate state $|E_g;el\rangle \otimes |E_{ex};phonon\rangle$, which can be reached via a DPP-mediated transition. It corresponds to the energy relaxation from the bottom of the conduction band ($E_g = 1.14$ eV) to the state $|E_g;el\rangle \otimes |E_{ex};phonon\rangle$ (in this paper, the energy of this state was experimentally determined to be 0.94 eV). This transition is allowable via emission of a large number of phonons or via the emission of infrared light. However, the probability of the transition via phonon emission is small because the simultaneous emission of about 10 phonons is required at room temperature (thermal energy 25 meV). On the other hand, in the transition via infrared light emission, since the electronic state changes from $|E_{ex};el\rangle$ to $|E_g;el\rangle$, the selection rule required for photon emission is fulfilled. In addition, this transition is a direct transition in wavenumber space, as shown in Figure 1(b). Therefore, the probability of this transition is higher than the probability of a transition via phonon emission. In real space, this process is a transition from the state $|E_{ex};el\rangle \otimes |E_{ex_{thermal}};phonon\rangle$, which is broadened to the extent of the electron coherence length, to the localized state $|E_g;el\rangle \otimes |E_{ex};phonon\rangle$. The reason why infrared light can be emitted in this transition is that part of the electron energy can be dissipated as infrared light via a DPP having an energy that is resonant with this infrared light.

Process (0′) is the second-step transition from the intermediate state $|E_g;el\rangle \otimes |E_{ex};phonon\rangle$ to $|E_g;el\rangle \otimes |E_{ex_{thermal}};phonon\rangle$. The photon energy emitted during this process is equal to $h\nu_{anneal}$. Since this is a transition between the same electronic states $|E_g;el\rangle$, the selection rule required for photon emission is governed by a phonon, and the state $|E_g;el\rangle \otimes |E_{ex};phonon\rangle$ is also a state that can be reached via a DPP-meditated transition. The Si-LED fabricated by DPP-assisted annealing has a high probability of conversion from a DPP to propagating light, and almost all of the electrons in the state $|E_g;el\rangle \otimes |E_{ex};phonon\rangle$ relax by emitting photons with energy $h\nu_{anneal}$.

Process (1) is the second-step transition from the intermediate state $|E_g;el\rangle \otimes |E_{ex};phonon\rangle$ to the final state $|E_g;el\rangle \otimes |E_{ex_{thermal}};phonon\rangle$ by absorption of an optical phonon. Since the first-step transition due to process (0) is an infrared light emission process, optical phonons are created via the Raman process. If the electrons in the state $|E_g;el\rangle \otimes |E_{ex};phonon\rangle$ are scattered to the Γ point by absorbing optical phonons, the second step transition from the state $|E_g;el\rangle \otimes |E_{ex'};phonon\rangle$ to the state $|E_g;el\rangle \otimes |E_{ex_{thermal}};phonon\rangle$ becomes possible, resulting in photon emission, as in the case of a direct transition-type semiconductor. This is process (1) shown in Figure 1(b). Here, $|E_{ex};phonon\rangle$ and $|E_{ex'};phonon\rangle$ are the excited states that the phonon reached before and after absorbing optical phonons. The energy of the emitted photons is $h\nu_{anneal} + h\nu_p$, where $h\nu_p$ is the energy of the optical phonon.

Process (1†) represents the second-step transition from the intermediate state $|E_g;el\rangle \otimes |E_{ex};phonon\rangle$ to the final state

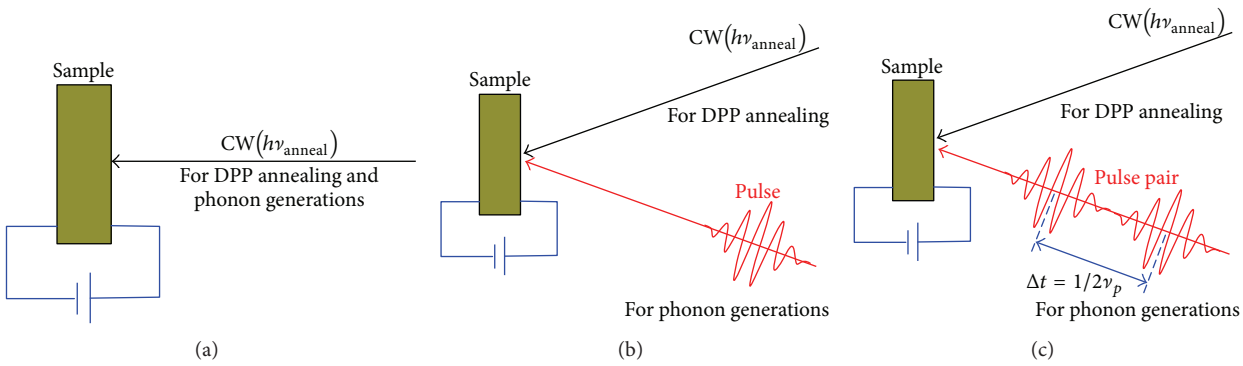

FIGURE 2: Illustration of DPP-assisted annealing using (a) CW light (conventional process); (b) CW light and a light pulse; and (c) CW light and two light pulses.

$|E_g; \text{el}\rangle \otimes |E_{\text{ex}_{\text{thermal}}}; \text{phonon}\rangle$, which occurs via emission of an optical phonon. Thus, it is conjugate to process (1). In this process, $|E_{\text{ex}''}; \text{phonon}\rangle$ in Figure 1 shows the phonon excited state after the emission of the optical phonon. The emitted photon energy is $h\nu_{\text{anneal}} - h\nu_p$.

Similarly, processes (n) and $(n^{\dagger})$ are transitions in which n optical phonons are absorbed or emitted. Since, in practice, the processes (n) and $(n^{\dagger})$ occur simultaneously, sidebands with photon energies $h\nu_{\text{anneal}} - nh\nu_p$ and $h\nu_{\text{anneal}} + nh\nu_p$ appear in the emission spectrum. The relationship between the nth order sideband energy and the photon energy $h\nu_{\text{anneal}}$ is the same as that of an nth order Raman scattering process with respect to the zero-phonon line. As is well-known, in Raman scattering, when a large number of phonons are excited, the electrons absorb them, emitting light. On the other hand, when a small number of phonons are excited, the electrons emit phonons, emitting light [17]. Thus, the intensity of these sidebands changes according to the number of phonons. This suggests that the intensity of the sidebands can be controlled by controlling the number of phonons.

3. Principle of Controlling the Number of Phonons

The number of created phonons can be controlled by a method involving multiphoton absorption or coherent phonon (CP) excitation using pulsed light. Since the Si crystal is heated by DPP-assisted annealing in the present work, resonant absorption to a specific exciton state for creation of coherent phonons is not possible by using a high-power CW-laser optical source. This is because the high-power CW laser excitation dose not change only the phonon structures but also DP state. Therefore, we decided to selectively create phonons via CP excitation using ultrashort pulsed light. The principle of the CP excitation in this case can be understood as an impulsive stimulated Raman scattering (ISRS) process, which is a kind of stimulated Raman scattering [18]. The duration and the repletion rate of the used pulsed light were 17 fs and 80 MHz, respectively. Therefore, its duty ratio was 1.3×10^{-6}. The Raman process is based on the third order optical nonlinearity. Therefore, the enough laser power for the control of CP generation using the ultrashort pulsed light is 2.3×10^{-18} times lower than that using the CW laser. Thus, in the experiment, the adverse effect was reduced to the negligible small coming from the DP generation by the additional laser excitation for the CP control.

In ISRS, the frequency component of the pulsed light irradiating the crystal includes coherent frequency components ν and $\nu - \nu_p$ with sufficiently high intensity, where ν_p is the phonon vibration frequency. Therefore, when the crystal is irradiated with pulsed light, the electrons absorb light with energy $h\nu$ and exhibit stimulated emission of light with energy $h\nu - h\nu_p$. At this time, it is possible to create CPs having an energy $h\nu_p$. Since these CPs are coherent, it is possible to control the creation of CPs by a single pulse or multiple pulses of light and causing them to interfere. In other words, unlike conventional DPP-assisted annealing in which the Si crystal is irradiated with CW light, CP creation is controlled by irradiating the Si crystal with pulsed light in addition to CW light. Therefore, it is possible to control the intensities of the sidebands in the EL spectrum. In the following, we describe the case where the Si-LED is irradiated with a single pulse of light during the DPP-assisted annealing and the case where the Si-LED is irradiated with a pair of light pulses.

(1) Irradiation with a Single Light Pulse. In the conventional DPP-assisted annealing, as shown in Figure 2(a), the CW light plays the role of decreasing the thermal diffusion rate by means of stimulated emission. In our approach, as shown in Figure 2(b), a light pulse is also radiated, together with the CW light. Since the light pulse excites multimode CPs via ISRS, the coupling probability of electron-hole pairs, photons, and CPs increases. As a result, the probability of electrons absorbing phonons and emitting light increases because the number of excited phonons increases as the light emission intensity increases. Therefore, the intensity of the sidebands having energy $h\nu_{\text{anneal}} + nh\nu_p$ increases, and the intensity of sidebands having energy $h\nu_{\text{anneal}} - nh\nu_p$ decreases. Thus, compared with an Si-LED fabricated by irradiation with only CW light, it is expected that the EL spectral shape of the Si-LED will show a higher light emission intensity at energies higher than $h\nu_{\text{anneal}}$ and conversely a lower light emission intensity at energies lower than $h\nu_{\text{anneal}}$.

(2) Irradiation with Two Light Pulses (Light Pulse Pair). Since the CPs created by ISRS are coherent and thus have the ability

to interfere, as described above, let us consider the case where a Si crystal is sequentially irradiated with two coherent light pulses having an arrival time difference Δt. If the value of Δt is a half-integer multiple of the vibration period, $1/\nu_p$, of the phonons ($n/2\nu_p$; $n = 1, 3, 5, \ldots$), as shown in Figure 2(c), it is known that the excited CPs destructively interfere [19]. On the other hand, they constructively interfere when Δt is an integer multiple of the vibration period (n/ν_p; $n = 1, 2, 3, \ldots$). That is to say, by radiating a pair of light pulses, it is possible to control the creation of CPs so as to be suppressed or enhanced. Thus, by adjusting the value of Δt, it is possible to perform various types of sideband control as compared with (1) above.

As an example, in the case of $\Delta t = 1/2\nu_p$, we will explain how the CP creation is controlled and how, as a result of this, the EL spectrum is controlled. The value $\Delta t = 1/2\nu_p$ corresponds to one period of vibration of a phonon with frequency $2\nu_p$. Therefore, by radiating a pair of pulses having this value Δt, the number of phonons of frequency ν_p decreases, whereas the number of phonons of frequency $2\nu_p$ increases. Thus, the probability of process ($1^\dagger$) increases, by which electrons emit phonons of frequency ν_p and emit light, resulting in a higher probability of electrons absorbing phonons of frequency $2\nu_p$ and emitting light. In other words, as a result of the reduction in the number of phonons with frequency ν_p, the intensity of the sideband at energy $h\nu_{\text{anneal}} - h\nu_p$ becomes higher than that of the sideband at energy $h\nu_{\text{anneal}} + h\nu_p$. At the same time, as a result of the increase in the number of phonons with frequency $2\nu_p$, the intensity of the sideband at energy $h\nu_{\text{anneal}} - 2h\nu_p$ becomes lower than that of the sideband at energy $h\nu_{\text{anneal}} + 2h\nu_p$. The above discussion can also be extended to an explanation of the case where the sideband intensity at energy $h\nu_{\text{anneal}} - (2n-1)\nu_p$ increases, and that at energy $h\nu_{\text{anneal}} + (2n-1)\nu_p$ decreases. It can be also extended to the case where the sideband intensity at energy $h\nu_{\text{anneal}} - 2n\nu_p$ decreases, and that at energy $h\nu_{\text{anneal}} + 2n\nu_p$ increases. For controlling the number of phonons during the DPP-assisted annealing, we irradiate two light pulses with delay times of $\Delta t = 1/\nu_{p,\text{exp}}$ (= 64.1 fs), $1/2\nu_{p,\text{exp}}$ (= 32.1 fs), and $1/4\nu_{p,\text{exp}}$ (= 16.0 fs).

4. Fabrication of Si-LED and Evaluation of EL Spectrum

To fabricate a Si-LED, we doped a 625 μm-thick n-type Si (100) substrate with arsenic (As) at a concentration of about 10^{15} cm^{-3}. The resulting resistivity was 10 Ωcm. Next, we formed a p-n homojunction by ion implantation of boron (B) with a dose of 5×10^{13} cm^{-2} and an acceleration energy of 700 keV. Then, we deposited a transparent ITO film with a thickness of 150 nm on the surface of the p layer and a Cr/Al film with a thickness of 80 nm on the surface of the n layer, both by RF sputtering, to form an anode and a cathode, respectively. The device fabrication conditions up to this point were the same as those reported in [12]. In DPP-assisted annealing, we used CW laser light with energy $h\nu_{\text{anneal}} = 0.94$ eV (wavelength 1.3 μm) as the light source for creating DPs. As the pulsed light source for creating CPs, we used a mode-locked laser with a photon energy of 1.55 eV (wavelength 0.8 μm), a pulse width of 17 fs, and a repetition frequency of 80 MHz. To verify the DPP-assisted annealing method, we employed the following four samples.

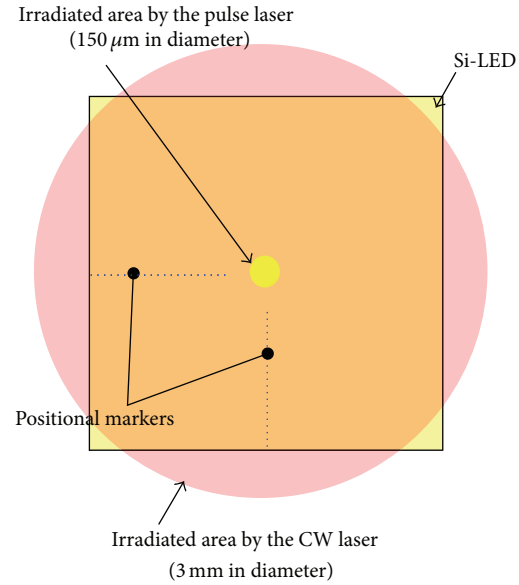

FIGURE 3: Irradiation spots of CW light and pulsed light on sample surface during DPP-assisted annealing.

(a) Sample 1. Sample 1 was irradiated with pulsed light (average power 100 mW, spot diameter 150 μm) and CW light ($h\nu_{\text{anneal}} = 0.94$ eV, power 1 W, spot diameter 3 mm). It was annealed with a voltage of 20 V and a current of 145 mA for 1 hour (Figure 2(b)).

(b) Samples 2–4. Of the CPs created by pulsed light irradiation, we selected optical phonons with the highest creation probability [20] ($h\nu_p = 65$ meV ($\nu_p = 15.6$ THz); indicated as $h\nu_{p,\text{exp}}$ below) as the phonons to be controlled. The samples were irradiated with CW light and a pair of light pulses with $\Delta t = 1/\nu_{p,\text{exp}}$ (= 64.1 fs), $1/2\nu_{p,\text{exp}}$ (= 32.1 fs), and $1/4\nu_{p,\text{exp}}$ (= 16.0 fs). They were annealed with a voltage of 25 V and a current of 120 mA for 1 hour (Figure 2(c)). The other experimental conditions were the same as those used for Sample 1 above. In the following, samples for $\Delta t = 1/\nu_{p,\text{exp}}$, $1/2\nu_{p,\text{exp}}$, and $1/4\nu_{p,\text{exp}}$ are referred to as Samples 2, 3, and 4, respectively.

To eliminate the contributions of variations in the sizes and shapes of the electrode and the substrate to the experimental results, the CW light was radiated onto the entire surface of the sample, and the pulsed light was radiated only at the center of the region irradiated with the CW light, as shown by the red and yellow circles, respectively, in Figure 3. With the samples prepared with this method, the EL spectral shapes in these two circles were different. By taking this difference between the intensities of these EL spectra, it was possible to eliminate the contributions above and to examine the details of the changes in the EL spectra depending on the presence/absence of the pulsed light irradiation. Experimental results are shown below.

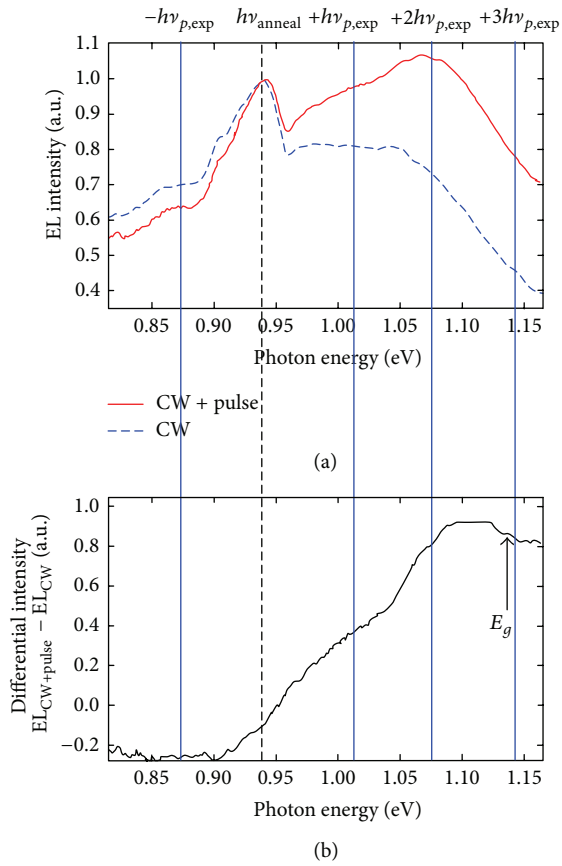

FIGURE 4: (a) EL spectra of Sample 1 after DPP-assisted annealing with the method in Figure 2(b). Red solid curve: area irradiated with CW light and pulsed light. Blue broken curve: area irradiated only with CW light. (b) Differential EL spectrum.

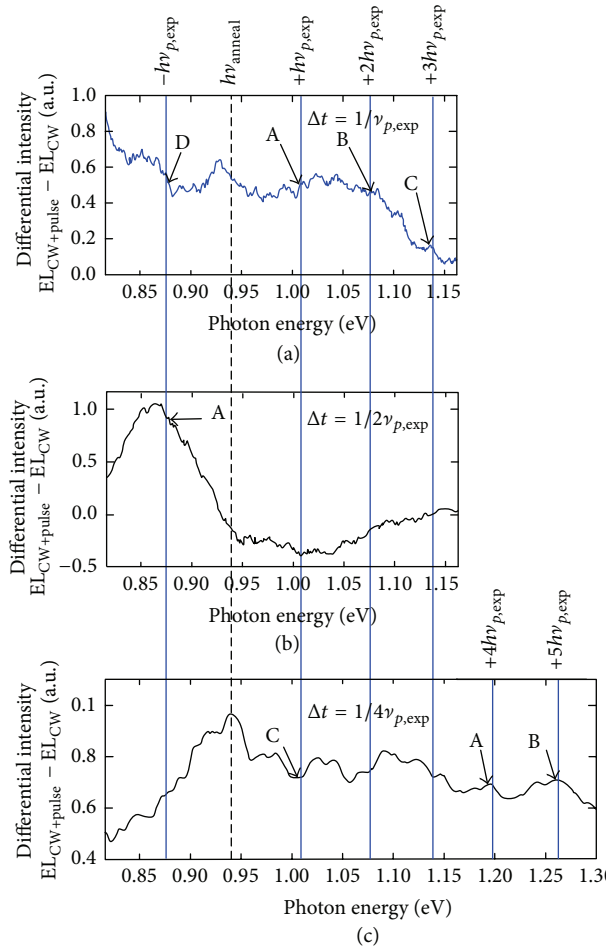

FIGURE 5: Differential EL spectra. (a) Sample 2 with $\Delta t = 1/\nu_{p,\exp}$. (b) Sample 3 with $\Delta t = 1/2\nu_{p,\exp}$. (a) Sample 4 with $\Delta t = 1/4\nu_{p,\exp}$.

(a) Sample 1. Figure 4(a) shows, for Sample 1, the EL spectrum of the part irradiated with only the CW light (blue broken curve: EL_{CW}) and the EL spectrum of the part irradiated with the CW light and the pulsed light (red solid curve: $\text{EL}_{\text{CW+pulse}}$). Figure 4(b) shows the difference between their intensities ($\text{EL}_{\text{CW+pulse}} - \text{EL}_{\text{CW}}$; differential EL spectrum). By irradiating the sample with the pulsed light, the EL intensity at higher energies increased, and the intensity of the +1 and +2 order sidebands of the optical phonons (energy $h\nu_{p,\exp}$ = 65 meV) increased. In the differential EL spectrum, we also confirmed band-edge light emission and an increase in the intensity of the +3 order sideband. However, since we did not perform mode selection by using a pair of pulses, the spectra of the sidebands were extremely broad. The increase in intensity of these sidebands is explained by the creation of a large number of CPs by ISRS, using the pulsed light, as explained in Section 3. In other words, since a large number of CPs are created, the process in which CPs are absorbed becomes dominant, resulting in light emission. In addition, the increase in light emission at the band edge is considered to be a consequence of the increased number of phonons due to CP creation causing an increased probability of a direct transition between electronic bands.

On the other hand, in the sideband corresponding to the −1 order optical phonons, the EL intensity is decreased by the incident pulsed light during DPP-assisted annealing. This is because process ($1^{\dagger}$), in which optical phonons and light are emitted, is suppressed due to CPs created by the pulsed light.

(b) Sample 2. Figure 5(a) shows the differential EL spectrum for Sample 2. In this sample, small bumps (arrows A, B, and C) are observed at the positions of the +1 to +3 order optical phonon sidebands ($h\nu_{p,\exp}$ = 65 meV). They are due to the selective creation of optical phonons $nh\nu_{p,\exp}$ ($n = 1, 2, 3, \ldots$), which were mode-selected by irradiating this sample with a pair of pulses with $\Delta t = 1/\nu_{p,\exp}$. On the other hand, a region with reduced light emission, like that seen in Figure 4(b), was not observed in the region whose energy is lower than $h\nu_{\text{anneal}}$ (arrow D). The reason for this is that the number of created optical phonons is half or less of that in the case of Sample 1 because ISRS is a second-order nonlinear process, and the energy of the pulses irradiating this sample is one-half of the energy of the pulses irradiating Sample 1. This is due to the

suppression of process ($1^{\dagger}$), in which light emission occurs while phonons are emitted.

(c) Sample 3. Figure 5(b) shows the differential EL spectrum for Sample 3. In this sample, the intensity of the −1 order sideband increased (arrow A). The reason for this is that, with $\Delta t = 1/2\nu_{p,\mathrm{exp}}$, the number of odd-numbered harmonic components was decreased, and the number of even-numbered harmonic components was increased. In other words, since the electrons had an increased probability of emitting the +1 order phonons, process ($1^{\dagger}$) was dominant, and the intensity of the −1 order sideband increased. On the other hand, process (1), in which light emission occurs while phonons are absorbed, is suppressed. Therefore, since the high-order modes are also suppressed, a region exhibiting reduced optical phonon sidebands is observed at energies higher than $h\nu_{\mathrm{anneal}}$, which is the opposite to what is shown in Figure 4(b).

(d) Sample 4. Figure 5(c) shows the differential EL spectrum for Sample 4. The intensities of the +1 order and +2 order sidebands were decreased, and those of the +4 order and +5 order sidebands were increased. A reason for this is that, with $\Delta t = 1/4\nu_{p,\mathrm{exp}}$, the number of +2 order harmonic phonons was decreased, and that the number of +4 order harmonic phonons was increased. The reason for the increase in the number of optical phonons in the +5 order is considered to be because the values of $1/4\nu_{p,\mathrm{exp}}$ and $1/5\nu_{p,\mathrm{exp}}$ are close. As a result, the intensity of the +1 order sideband is decreased. In other words, this is because the +1 order optical phonons are absorbed for creating the +4 order and +5 order harmonic phonons. The reason why the generation of the +5 order sideband dominates over generation of the +1 order sideband is that the energy of the +5 order sideband is higher than the bandgap energy, E_g, of Si, and this is a phonon scattering process that is resonant with the electronic level. As a result, process (1) is suppressed, and the intensity of the +1 order sideband is decreased. On the other hand, since the overall number of optical phonons is increased, process ($1^{\dagger}$) is suppressed, as in the case of Figure 4(b). As a result, a region with reduced light emission, similar to that seen in Figure 4(b), is observed in the region at energy $h\nu_{\mathrm{anneal}} - nh\nu_{p,\mathrm{exp}}$.

Figure 6 shows EL spectra of the regions irradiated with the light pulses for Samples 2 and 3. In Sample 2, the numbers of phonons of the fundamental ($h\nu_{p,\mathrm{exp}}$) and the harmonics ($nh\nu_{p,\mathrm{exp}}$; $n = 2, 3, \ldots$) were all increased, and therefore, the phonon absorption probability of the electrons increased, resulting in higher light emission at higher energies. In Sample 3, on the other hand, due to the interference of CPs, the number of odd-order harmonic components of the phonons was decreased, and the number of even-order harmonic components was increased; therefore, the absorption probability of phonons of odd-order harmonic components was decreased, resulting in relatively higher light emission at lower energies. The above results indicate that the EL spectral shape of the Si-LED was successfully controlled by changing the conditions of the pair of light pulses radiated during DPP-assisted annealing. That is, the intensity at energies higher than $h\nu_{\mathrm{anneal}}$ is increased, and that at lower energies is decreased. Furthermore, conversely, the intensity at energies lower than $h\nu_{\mathrm{anneal}}$ is increased, and that at higher energies is decreased.

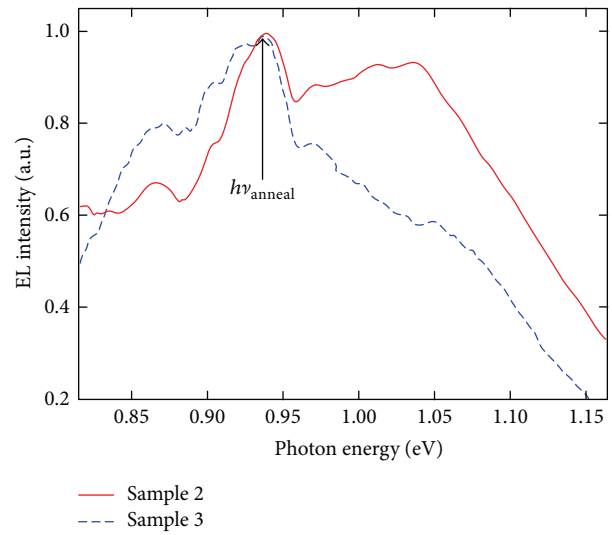

FIGURE 6: EL spectra after annealing for Samples 2 and 3.

In DPP-assisted annealing without using a pulsed light source, the broadening (half width at half maximum, HWHM) towards lower energies was 250 meV or greater, and the broadening (HWHM) towards higher energies was 50 meV. In contrast, in the EL spectrum of the Si-LED fabricated using a pulsed light source for creating phonons, the EL spectrum was broadened towards higher energies by 200 meV or greater (HWHM), and the broadening towards lower energies was reduced to 120 meV (HWHM).

5. Conclusion

In DPP-assisted annealing, we successfully controlled the spectral shape of a Si LED by radiating a pair of light pulses for creating CPs. In the EL spectrum, the intensity of sidebands due to phonons could be controlled by the number of phonons during DPP annealing. The peak wavelength in the EL spectrum was determined by the wavelength of the light source used in DPP-assisted annealing. In order to broaden the EL spectrum toward higher energy, a pair of light pulses having $\Delta t = 1/4\nu_{p,\mathrm{exp}}$ was radiated. Conversely, to broaden the EL spectrum towards lower energies, a pair of light pulses having $\Delta t = 1/2\nu_{p,\mathrm{exp}}$ was radiated. As a result, the EL spectrum was broadened towards higher energies by 200 meV or greater (HWHM), and the broadening towards lower energies was reduced to 120 meV (HWHM).

Conflict of Interests

The authors declare that there is no conflict of interests regarding the publication of this paper.

References

[1] Z. I. Alferov, "The history and future of semiconductor heterostructures," *Semiconductors*, vol. 32, no. 1, pp. 1–14, 1998.

[2] R. A. Milano, P. D. Dapkus, and G. E. Stillman, "An analysis of the performance of heterojunction for fiber optic communications," *IEEE Transactions on Electron Devices*, vol. 29, no. 2, pp. 266–274, 1982.

[3] National Toxicology Program, "NTP technical report on the toxicology and carcinogenesis studies of indium phosphide (CAS No. 22398-80-7) in F344/N rats and B6C3F1 mice (inhalation studies)," Tech. Rep. NTP TR 499, U.S. Department of health and human services, Public Health Service, National Institute of Health, 2001.

[4] K. D. Hirschman, L. Tsybeskov, S. P. Duttagupta, and P. M. Fauchet, "Silicon-based visible light-emitting devices integrated into microelectronic circuits," *Nature*, vol. 384, no. 6607, pp. 338–341, 1996.

[5] Z. H. Lu, D. J. Lockwood, and J.-M. Baribeau, "Quantum confinement and light emission in SiO_2/Si superlattices," *Nature*, vol. 378, no. 6554, pp. 258–260, 1995.

[6] L. Dal Negro, R. Li, J. Warga, and S. N. Basu, "Sensitized erbium emission from silicon-rich nitride/silicon superlattice structures," *Applied Physics Letters*, vol. 92, no. 18, Article ID 181105, 2008.

[7] T. Komoda, J. Kelly, F. Cristiano et al., "Visible photoluminescence at room temperature from microcrystalline silicon precipitates in SiO2 formed by ion implantation," *Nuclear Instruments and Methods in Physics Research B*, vol. 96, no. 1-2, pp. 387–391, 1995.

[8] S. Yerci, R. Li, and L. Dal Negro, "Electroluminescence from Er-doped Si-rich silicon nitride light emitting diodes," *Applied Physics Letters*, vol. 97, no. 8, Article ID 081109, 2010.

[9] S. K. Ray, S. Das, R. K. Singha, S. Manna, and A. Dhar, "Structural and optical properties of germanium nanostructures on Si(100) and embedded in high-k oxides," *Nanoscale Research Letters*, vol. 6, no. 1, article 224, 10 pages, 2011.

[10] M. A. Green, J. Zhao, A. Wang, P. J. Reece, and M. Gal, "Efficient silicon light-emitting diodes," *Nature*, vol. 412, no. 6849, pp. 805–808, 2001.

[11] T. Kawazoe, K. Kobayashi, S. Takubo, and M. Ohtsu, "Nonadiabatic photodissociation process using an optical near field," *Journal of Chemical Physics*, vol. 122, no. 2, Article ID 024715, 2005.

[12] T. Kawazoe, M. A. Mueed, and M. Ohtsu, "Highly efficient and broadband Si homojunction structured near-infrared light emitting diodes based on the phonon-assisted optical near-field process," *Applied Physics B*, vol. 104, no. 4, pp. 747–754, 2011.

[13] T. Kawazoe, M. Ohtsu, K. Akahane, and N. Yamamoto, "Si homojunction structured near-infrared laser based on a phonon-assisted process," *Applied Physics B: Lasers and Optics*, vol. 107, pp. 659–663, 2012.

[14] H. Tanaka, T. Kawazoe, and M. Ohtsu, "Increasing Si photodetector photosensitivity in near-infrared region and manifestation of optical amplification by dressed photons," *Applied Physics B*, vol. 108, no. 1, pp. 51–56, 2012.

[15] N. Wada, T. Kawazoe, and M. Ohtsu, "An optical and electrical relaxation oscillator using a Si homojunction structured light emitting diode," *Applied Physics B: Lasers and Optics*, vol. 108, no. 1, pp. 25–29, 2012.

[16] M. A. Tran, T. Kawazoe, and M. Ohtsu, "Fabrication of a bulk silicon p-n homojunction-structured light-emitting diode showing visible electroluminescence at room temperature," *Applied Physics A: Materials Science and Processing*, vol. 115, no. 1, pp. 105–111, 2014.

[17] S. K. Arora, A. J. Kothari, R. G. Patel, K. M. Chauha, and B. N. Chudasama, "Optical absorption in gel grown cadmium tartrate single crystals," *Journal of Physics*, vol. 28, no. 1, pp. 48–52, 2006.

[18] Y.-X. Yan, E. B. Gamble Jr., and K. A. Nelson, "Impulsive stimulated scattering: general importance in femtosecond laser pulse interactions with matter, and spectroscopic applications," *The Journal of Chemical Physics*, vol. 83, no. 11, pp. 5391–5399, 1985.

[19] M. Hase, K. Mizoguchi, H. Harima et al., "Optical control of coherent optical phonons in bismuth films," *Applied Physics Letters*, vol. 69, no. 17, pp. 2474–2476, 1996.

[20] P. Giannozzi, S. de Gironcoli, P. Pavone, and S. Baroni, "Ab initio calculation of phonon dispersions in semiconductors," *Physical Review B*, vol. 43, no. 9, pp. 7231–7242, 1991.